

Experimental study on negative effective mass in a 1D mass–spring system

Shanshan Yao, Xiaoming Zhou and Gengkai Hu¹

School of Science, Beijing Institute of Technology, Beijing 100081,
People's Republic of China
E-mail: hugeng@bit.edu.cn

New Journal of Physics **10** (2008) 043020 (11pp)

Received 25 January 2008

Published 14 April 2008

Online at <http://www.njp.org/>

doi:10.1088/1367-2630/10/4/043020

Abstract. A mass–spring system with negative effective mass is experimentally realized, and its transmission property is examined in the low-frequency range. The local resonance of the basic unit is observed and explained by Newton's theory. The negative effective mass is confirmed by experiments through the transmission properties of a finite periodic system composed of such basic units. In the negative mass range, low transmissions of the system are observed and it is well predicted by the theory. In addition, zero effective mass is discussed and experimentally investigated, which gives rise to no phase shifts in the system. Finally, the anti-vibration effect with a negative mass system is also analyzed. The relevant results are helpful for a better understanding of the resonant nature of metamaterials.

¹ Author to whom any correspondence should be addressed.

Contents

| | |
|--|-----------|
| 1. Introduction | 2 |
| 2. Theoretical analysis | 3 |
| 3. Experimental results | 4 |
| 4. Zero effective mass | 7 |
| 5. Applications and discussions | 8 |
| 6. Conclusions | 10 |
| Acknowledgments | 11 |
| References | 11 |

1. Introduction

Under external stimulations, most natural materials react in phase with the excitation. However by carefully designing microstructures, a class of composites can be fabricated to react out of phase with the external excitation due to resonant mechanism. These materials with unusual responses have been classified as metamaterials, such as periodic wires [1] and split ring resonators [2] in electromagnetics, as well as the locally resonant phononic crystals [3] and the periodic Helmholtz resonant cavities [4] in acoustics. The material parameters of metamaterials can be tuned to any values in material space by adjusting the microstructures. As an example, locally resonant phononic crystals can exhibit negative mass density [5] at the frequencies where sub-wavelength microstructures resonate and move out of phase with the excitation. Recently, rigorous definitions of effective mass density for particle or fiber filled metamaterials have been discussed with multiple scattering theory [6, 7].

Negative mass density can also be realized by a simple mass–spring system [8, 9]. Milton and Willis [10] examined the microstructures giving rise to negative effective mass. They suggested that the dynamic effective mass of composite materials should be defined in the framework of Newton’s law of motion, contrary to the static gravitational mass. Their studies reveal that composite materials with carefully designed microstructures can have a *negative-momentum* for a *positive-momentum* excitation, thus characterized by the negative effective mass. Although many theoretical works are devoted to discuss the negative effective mass, however the corresponding experimental studies devoting to illustrate the intrinsic mechanism are few.

In this work, we will experimentally examine the composite system proposed by Milton and Willis [10] in the low frequency regime. Contrary to high frequency or ultrasonic experiments [3, 11], low frequency experiments are more suitable to illustrate the underlying mechanism of basic properties, since the movement of microstructures can be well observed and determined experimentally. The paper is arranged as follows: we will first recall the model proposed by Milton and Willis in section 2. Experiments will be set-up to characterize the dynamic response of the model. The transmission properties of a one-dimensional (1D) finite periodic system will be determined. The relevant analyses will be given in section 3. An interesting phenomenon induced by zero effective mass will be discussed in section 4. In section 5, the anti-vibration design of a finite system with negative effective mass is experimentally analyzed and discussed. The paper ends with some conclusions and remarks.

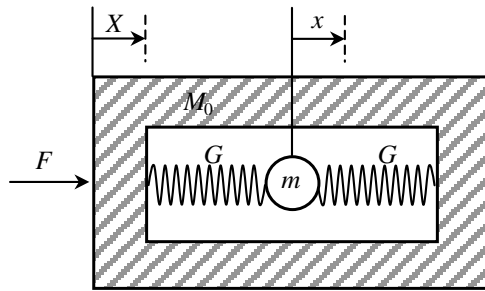


Figure 1. 1D model with negative effective mass.

2. Theoretical analysis

The basic unit is shown in figure 1. A rigid bar of mass M_0 has a cavity to connect it to a rigid sphere of mass m by two massless and elastic springs with equal constant G . The rigid bar together with the internal sphere and springs is equivalent to a solid object with an effective mass (or p-mass) $M_{\text{eff}}^{\text{P}}$; both have the same momentum. Under a time harmonic excitation $e^{-i\omega t}$, the displacement relation between the rigid sphere and bar is given by [10]

$$\frac{x}{X} = \frac{2G}{2G - m\omega^2}, \quad (1)$$

where x and X are the displacement amplitudes of the sphere and bar, respectively. The effective mass $M_{\text{eff}}^{\text{P}}$ of the unit is defined as the total momentum divided by the bar velocity, this leads to [10]

$$M_{\text{eff}}^{\text{P}} = M_0 + \frac{m\omega_0^2}{\omega_0^2 - \omega^2}, \quad (2)$$

where $\omega_0 = \sqrt{2G/m}$ is the resonant frequency. The expression of $M_{\text{eff}}^{\text{P}}$ is analogous to the Lorentz model for electromagnetic metamaterials [12]. Therefore the basic unit shown in figure 1 shares some similarities with electromagnetic metamaterials. In this sense, the momentum is analogous to electric or magnetic polarizations and the velocity is analogous to electric or magnetic fields. Equation (2) shows that the effective mass $M_{\text{eff}}^{\text{P}}$ can be negative in the frequency band from ω_0 to $\omega_0\sqrt{(M_0+m)/M_0}$. The negativity of the effective mass comes from the negative momentum of the sphere, since it can move out of phase with respect to the bar after resonance. However, the energy of the unit cannot be simply defined with the effective p-mass and bar velocity V as $E = M_{\text{eff}}^{\text{P}}|V|^2/2$, since the kinetic energy must be positive even in the negative mass band.

In the actual case, the negative mass of the analyzed model cannot be measured directly. As a common and indirect method, an infinite 1D periodic mass–spring system can be constructed with the basic units described previously connected with equal springs of constant K , as shown in figure 2. By evaluating the dispersion relation and transmission properties of the whole system, the frequency-dependent properties of each unit can be determined. A spacing a between two adjacent units is assumed. From Newton's law of motion, the total momentum P of the n th unit satisfies the following equation, where X_n is the displacement of the n th unit

$$\frac{dP}{dt} = K(X_{n+1} - X_n) + K(X_{n-1} - X_n). \quad (3)$$

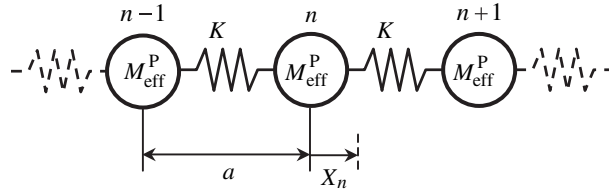


Figure 2. An infinite periodic mass–spring system.

For a harmonic field, this leads to

$$-\omega^2 M_{\text{eff}}^P X_n = K (X_{n+1} + X_{n-1} - 2X_n). \quad (4)$$

According to the Bloch's theorem [13, 14] and periodic boundary conditions, the displacement of each unit can be represented by $X_n = A e^{i(qna - \omega t)}$, where q is the Bloch wavevector. From (4), we get the dispersion-like relation for the infinite periodic system

$$M_{\text{eff}}^P \omega^2 = 4K \sin^2 \frac{qa}{2}. \quad (5)$$

For a finite periodic system counting N units, the transmission of the system can be derived analytically. The displacement of the unit is supposed to be $X_n(t) = \bar{X}_n e^{-i\omega t}$, where \bar{X}_n is the time-independent complex displacement. Then it is easy to obtain the following relations:

$$(2K - \omega^2 M_{\text{eff}}^P) \bar{X}_n = K (\bar{X}_{n+1} + \bar{X}_{n-1}), \quad n = 1, 2, \dots, N-1; \quad (6a)$$

$$(K - \omega^2 M_{\text{eff}}^P) \bar{X}_n = K \bar{X}_{n-1}, \quad n = N. \quad (6b)$$

From (6), the transmittance $T = |\bar{X}_N / \bar{X}_0|$ of the finite periodic system is

$$T = \left| \prod_{n=1}^N T_n \right|, \quad (7)$$

where $T_n = \bar{X}_n / \bar{X}_{n-1}$ is given by the following recurrent relation:

$$T_n = \frac{K}{K(2 - T_{n+1}) - M_{\text{eff}}^P \omega^2}, \quad n = 1, 2, \dots, N, \quad (8)$$

with $T_{N+1} = 1$.

3. Experimental results

To verify the frequency-dependent effective mass of the studied model, we conduct 1D experiments for the mass–spring system analyzed previously. In the experiment, we place the samples in the horizontal direction. In order to eliminate the friction of the system during the movement, an air track with triangular cross-section is employed. The unit is made of aluminium blocks with Δ shape in the bottom to match the configuration of the air track. The upper surface of the track and the bottom of the blocks are perfectly matched to guide the unit in an accurate direction. When the air track is driven by an air pump, the tiny holes made on the surface of the track produce high-pressure air currents to lift the unit from the track. By this method, the contact friction can be efficiently reduced. Each unit is made of three blocks of length 30 mm, the first and last blocks are fixed together on the top by an aluminium sheet and the middle one

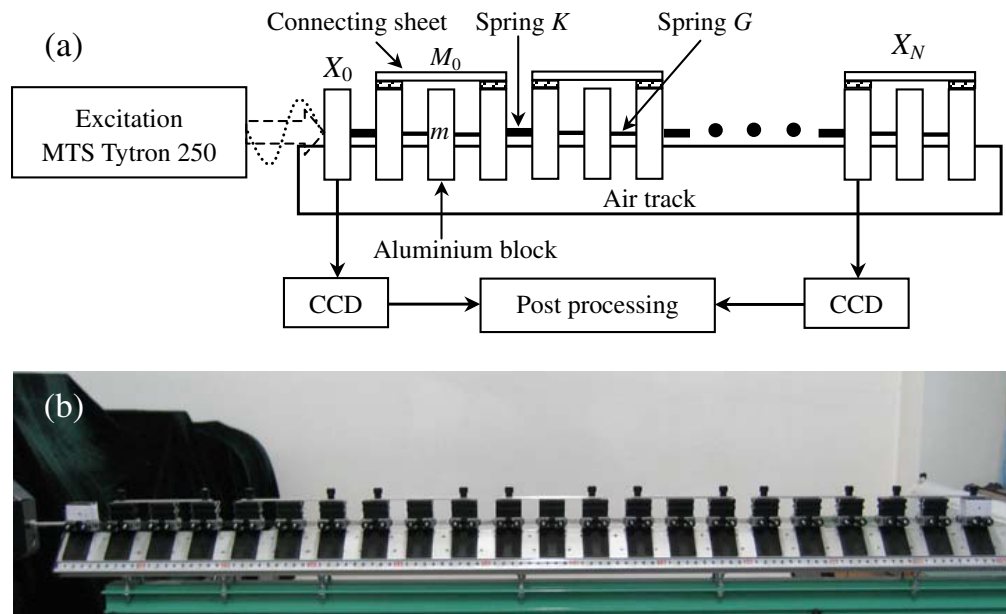


Figure 3. (a) Scheme and (b) actual picture of the experimental setup.

is free to move. The three blocks are connected to each other by two soft springs with the same spring constant 37 N m^{-1} . The connecting point of the spring is very close to the centroid of the block to make the stability in motion sure. The total weight of the outer connected blocks of each unit is $M_0 = 101.10 \text{ g}$, and the weight of the middle block is $m = 46.47 \text{ g}$. A time harmonic displacement is produced through MTS Tytron 250 as the excitation. The scheme of the system is shown in figure 3.

The displacements of M_0 and m in the model are measured with a CCD technique. The CCD camera captures pictures with a time interval of 7 ms. With this technique, we first measure the displacement relation of the masses M_0 and m for a single unit. The experimental result for the amplitude ratio $|x|/|X|$ are shown in figure 4, and they are compared with the theoretical prediction given by (1) in the frequency range below 12 Hz. An excellent agreement can be observed in the entire testing region. The result clearly shows that the displacement of m is greatly enhanced close to the resonant frequency. After experiencing the strong resonance, m always moves in the opposite direction with respect to M_0 . For this reason, the motion of m will be characterized by a negative momentum. This is also the underlying mechanism for negative effective mass. In the experiment, we perform the measurements many times and find that the experimental error is very small. The excellent correlation between the measured and theoretical results indicates that the influence of friction can be neglected and that the data acquisition method is reliable in this frequency regime.

For an infinite periodic system consisting of the prescribed models, substituting the experimental parameters into (5), we give the dispersion relation of the periodic system in figure 5(a) in the region below the *cut-off* frequency 12 Hz. It can be seen that negative effective mass of the units will lead to a band gap from about 5.8 to 7.6 Hz. It is evident that the gap is induced by the negative values of mass. This may be an indirect method to confirm the negative mass in experiments. However the dispersion curve is almost impossible to be examined experimentally, since the particle motion in an infinite 1D lattice is different from that

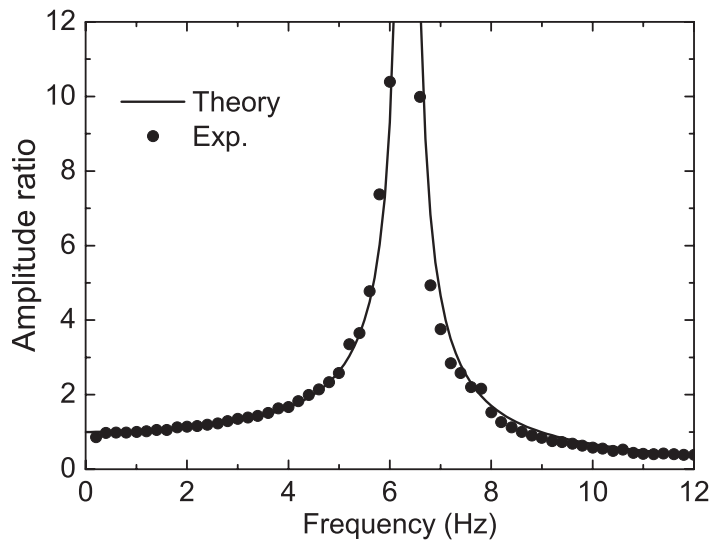


Figure 4. Ratio of displacement amplitudes $|x|/|X|$ between m and M_0 for one unit under a harmonic excitation.

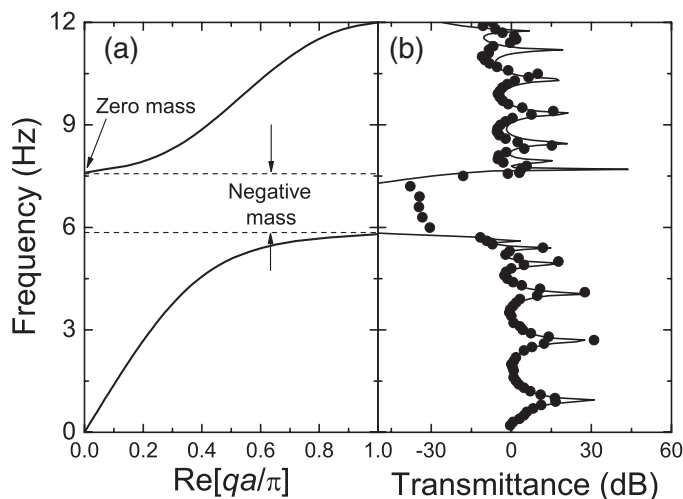


Figure 5. (a) The dispersion relation predicted by (5); (b) the experimental and theoretical transmittances of a finite system with seven units.

in a finite one [15] due to the different boundary conditions. However a correlation between the dispersion curve of an infinite system and macroscopic transmission property of a finite system still exists. From this consideration, we employ seven *negative-mass* units described above, which are connected to each other by springs of constant 117 N m^{-1} , to construct a finite periodic system. Note that the length of one period (composed of one unit and one spring) is 137 mm. Figures 3(a) and (b) show the schematic and actual pictures of the experimental set-up, respectively. The displacements X_0 and X_N of the excitation and the last unit are measured, respectively. Figure 5(b) gives the amplitude ratio of X_N/X_0 , defined as the transmittance of the finite system. As a comparison, the theoretical transmittance predicted by (7) is also depicted. Good agreement can be observed between the experimental and theoretical results in the whole

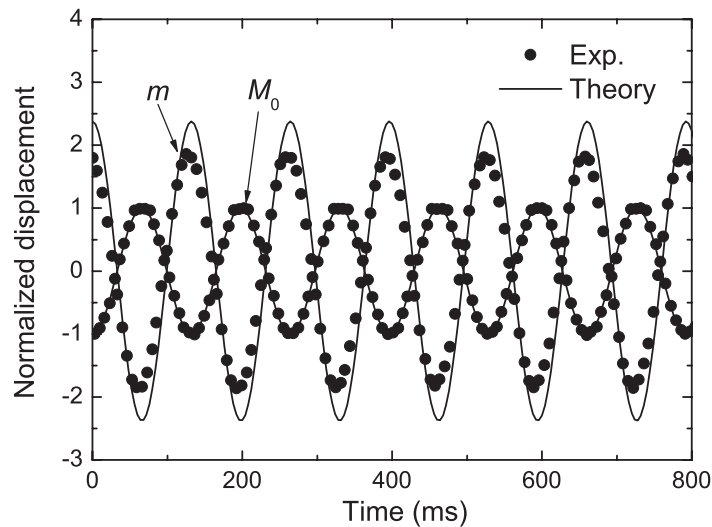


Figure 6. The experimental and theoretical displacement curves of m and M_0 at the frequency 7.57 Hz.

frequency range. In the band gap of the infinite periodic system as shown figure 5(a), the transmittance is less than -20 dB, which is clearly due to the negative p-mass of the constitutive units. In the gap, we observe that the vibration amplitude of M_0 decays rapidly almost within three periods, while the internal blocks m vibrate remarkably. Till now we can conclude that the negative effective mass can indeed be realized in a simple mass–spring model.

4. Zero effective mass

From (2), we can obtain the zero effective p-mass for the unit at the frequency $\omega = \omega_0 \sqrt{(M_0 + m)/M_0}$. In this situation, a simple relation $x/X = -M_0/m$ can be obtained from (1), which indicates that the total momentum of the unit is zero. The theoretical frequency of zero mass is predicted as 7.67 Hz for the unit. In the experiment, we take the measurements carefully at frequencies around 7.67 Hz and find that the amplitude ratio $x/X \approx 2.03$ at 7.57 Hz is the one, which is more close to $M_0/m \approx 2.17$ of the sample. We attribute this frequency shift to slight dissipation in the experimental system. When the dissipation is incorporated into the negative mass model, for example a dashpot component is considered (see equation 2.13 in [10]), the frequency corresponding to zero mass may be shifted by the additional dissipation term. In this experiment, the dissipation may be originated from the viscosity of springs, and the remaining contact frictions between samples and the track. For a single unit, the measured displacements of M_0 and m with respect to time together with the theoretical results at 7.57 Hz are shown in figure 6. A good correlation between experiment and theory can be found. Although the measured displacement of m has a little deviation with respect to the theory due to dissipation, it is clear that m always moves in the opposite direction of M_0 and that the total momentum of the unit is extremely small.

For a finite periodic system composed of *zero-mass* units (at the examined frequency), we conduct the experiment on a seven-unit system at the frequency 7.57 Hz. It is observed that at this frequency all units move in the same manner and the springs connecting units have no

deformations. The whole system reacts like a rigid bar experiencing no phase shift in the system. We know that the vanishing momentum of the *zero-mass* unit means its inertial force under the outside excitation is zero, so it seems like that the periodic system were composed of massless springs. In this sense, it is evident that the connecting springs will not deform and the whole system behaves like a rigid bar. Another explanation can also be given according to the lattice wave propagation in a periodic system. In (5), we can find that the wave vector q will be zero when the p-mass $M_{\text{eff}}^{\text{P}} = 0$. It is known that the wavevector characterizes the field distribution and spatial dispersion of propagating waves. The zero wavevector indicates that the wavelength of the propagating wave in the system is infinite and this means that there are no variations of the displacement fields in the system. This phenomenon corresponding to the zero p-mass is very similar to that occurring for electromagnetic waves propagating in a matched zero-index metamaterial [16], which has zero permittivity and permeability simultaneously. Inside this material, the electromagnetic fields have zero phase variations.

5. Applications and discussions

In this section, the anti-vibration by a negative mass system will be discussed. The previous experiments have revealed that vibrations can be stopped in the frequency range where the effective mass is negative, so it is natural to explore this property for anti-vibration design. Consider now a finite periodic system of N units, which is connected with a mass M_{L} by a spring K_{c} at the end of the system. The transmittance T of the whole system can be calculated by

$$T = \left| \prod_{n=1}^{N+1} T_n \right|, \quad (9)$$

where T_n is given by the following recurrent relation:

$$T_n = \frac{K}{K(2 - T_{n+1}) - M_{\text{eff}}^{\text{P}} \omega^2}, \quad n = 1, 2, \dots, N - 1, \quad (10)$$

with $T_N = \frac{K}{K_c(1 - T_{N+1}) + K - M_{\text{eff}}^{\text{P}} \omega^2}$ and $T_{N+1} = \frac{K_c}{K_c - M_{\text{L}} \omega^2}$.

A finite system with three periods is examined in the experiment, as shown in figure 7. The transmission property is first measured and compared with the theoretical prediction given by (7), which is shown in figure 8. We find that the correlation between the experiment and the prediction is very good and both results show a stop band from 6 to 7 Hz, at which the transmittance is around -20 dB in the experiment. In the following, we attach the previous system with a mass M_{L} by a spring K_{c} . By varying the values of M_{L} and K_{c} , we systematically evaluate the anti-vibration effect of this device. Four different cases are examined: (a) $M_{\text{L}} = 45.78$ g, $K_{\text{c}} = 37$ N m $^{-1}$, (b) $M_{\text{L}} = 45.78$ g, $K_{\text{c}} = 117$ N m $^{-1}$, (c) $M_{\text{L}} = 72.46$ g, $K_{\text{c}} = 37$ N m $^{-1}$ and (d) $M_{\text{L}} = 72.46$ g, $K_{\text{c}} = 117$ N m $^{-1}$. The theoretical predictions with (9) and experimental results for the transmittance as a function of frequency are shown in figure 9. Good agreements between the theoretical and experimental results for different cases can be observed. From figure 9, it can be seen that the stop band still exists for the examined cases, however the corresponding frequency range and amplitude of vibration have been modified a little, compared to the results without the attached mass. For the case of $M_{\text{L}} = 45.78$ g and $K_{\text{c}} = 37$ N m $^{-1}$, the vibration amplitude is beyond -20 dB in the band gap of the device, whereas the transmittance can still achieve -15 dB, as shown in figure 9(a). However when the connecting spring is

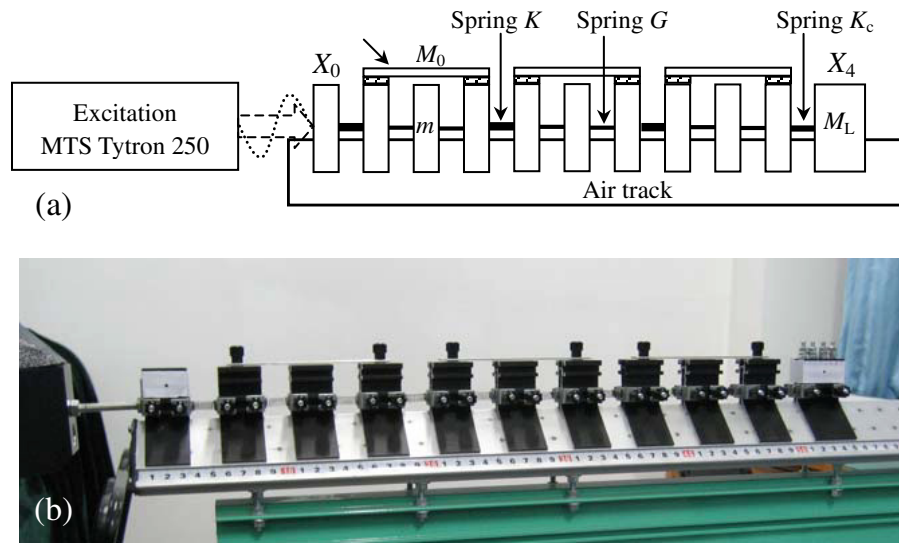


Figure 7. (a) Scheme and (b) actual picture of the anti-vibration experiment.

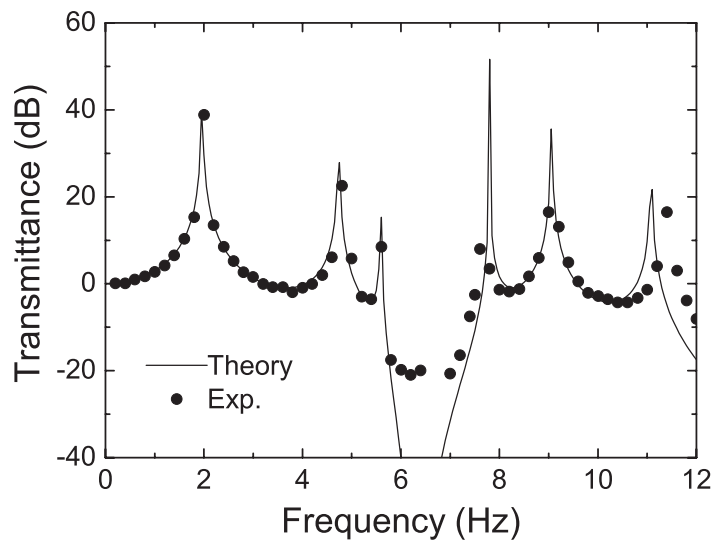


Figure 8. Experimental and theoretical transmittances for a three-unit system.

replaced by $K_c = 117 \text{ N m}^{-1}$, a pass band around 7 Hz takes place in the band gap (figure 9(b)), this is detrimental to the shielding effect of the device. When a relatively large mass $M_L = 72.46 \text{ g}$ is used, the band gap of the system is relatively insensitive to the connecting springs, as shown in figures 9(c) and (d). These results reveal that the anti-vibration design utilizing negative effective mass needs careful analysis of the whole system, in order to make an efficient anti-vibration device.

The anti-vibration effect presented above comes from the total reflection mechanism induced by negative mass. It is different from the transformation based acoustic cloaking in 2D [17, 18] and 3D [19, 20]. Based on the coordinate transformation method [21, 22], acoustic metamaterial with anisotropic mass density could guide waves around an object without any disturbance. It is worth to say that the negative mass model shown in figure 1 is important in

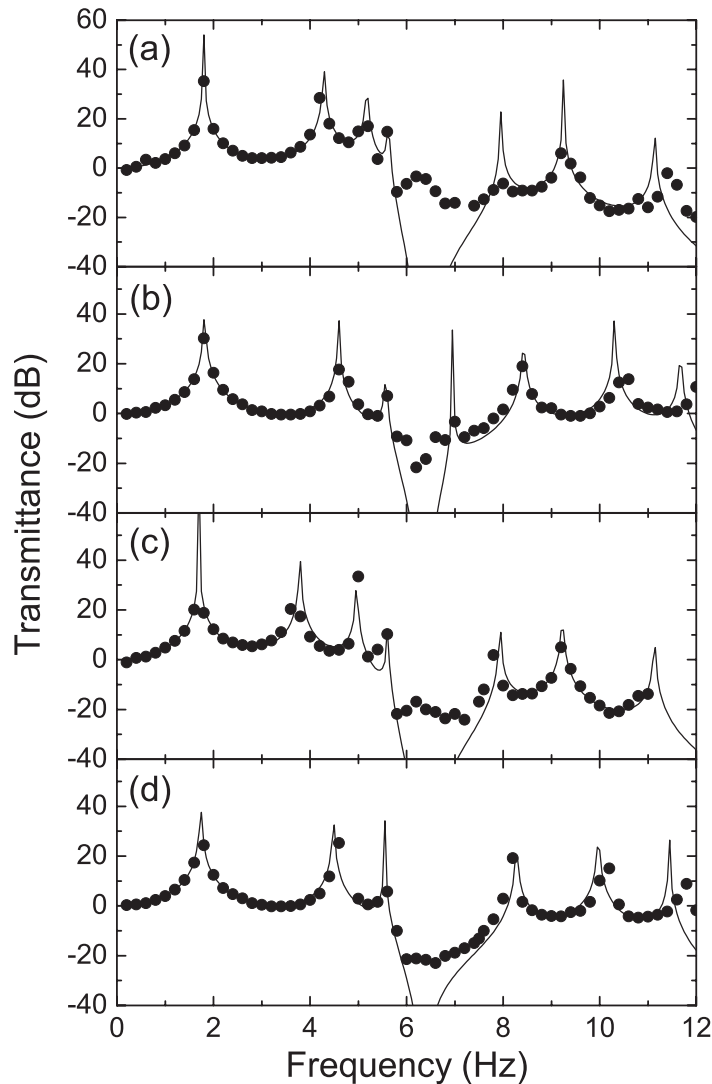


Figure 9. Experimental (black dot) and theoretical (solid line) transmittances for a three-unit system with an attached mass: (a) $M_L = 45.78$ g, $K_c = 37$ N m $^{-1}$; (b) $M_L = 45.78$ g, $K_c = 117$ N m $^{-1}$; (c) $M_L = 72.46$ g, $K_c = 37$ N m $^{-1}$ and (d) $M_L = 72.46$ g, $K_c = 117$ N m $^{-1}$.

realizing the acoustic cloak, since the model can be easily extended to 2D and 3D case so that the mass density has a matrix form, as indicated by Milton and Willis [10]. The periodic lattice structures made of mass and spring have been acting as a wave filter and wave guiding [23]. Thus the mass–spring cloak that shields objects from vibration can be anticipated with the help of the negative mass model.

6. Conclusions

In this paper, we have studied experimentally the mass–spring model proposed by Milton and Willis [10]. This system can have negative effective mass in the frequency band when the internal sphere moves out of phase with respect to the outer bar. For an indirect demonstration

of negative mass, a finite periodic system consisting of many units connected by elastic springs is constructed. By measuring the transmission curves of the system, the low transmission frequency range has been observed and it corresponds well to the stop band induced by the negative mass for an infinite system. In addition, zero effective mass is also examined. In the case of zero effective mass, the constructed finite system moves like a rigid bar, i.e. there is no phase shift in the system. This phenomenon is induced by the zero momentum of the model and can also be explained by the zero propagating vector in the system. Finally the anti-vibration effect is investigated by experiments with negative effective mass. The results presented in this paper may be helpful for understanding acoustic metamaterials in realizing negative parameters.

Acknowledgments

This work was supported by the National Natural Science Foundation of China (10325210, 90605001, 10702006), and the National Basic Research Program of China (2006CB601204). Dr Shaopeng Ma and Mr Qinwei Ma are acknowledged for data acquisition with the CCD technique.

References

- [1] Pendry J B, Holden A J, Robbins D J and Stewart W J 1996 *Phys. Rev. Lett.* **76** 4773
- [2] Pendry J B, Holden A J, Stewart W J and Youngs I 1999 *IEEE Trans. Microw. Theory Tech.* **47** 2075
- [3] Liu Z Y, Zhang X X, Mao Y W, Zhu Y Y, Yang Z Y, Chan C T and Sheng P 2000 *Science* **289** 1734
- [4] Fang N, Xi D, Xu J, Ambati M, Srituravanich W, Sun C and Zhang X 2006 *Nat. Mater.* **5** 452
- [5] Sheng P, Zhang X X, Liu Z Y and Chan C T 2003 *Physica B* **338** 201
- [6] Mei J, Liu Z Y, Wen W J and Sheng P 2006 *Phys. Rev. Lett.* **96** 024301
- [7] Mei J, Liu Z Y, Wen W J and Sheng P 2007 *Phys. Rev. B* **76** 134205
- [8] Hirsekorn M 2004 *Appl. Phys. Lett.* **84** 3364
- [9] Liu Z Y, Chan C T and Sheng P 2005 *Phys. Rev. B* **71** 014103
- [10] Milton G W and Willis J R 2007 *Proc. R. Soc. A* **463** 855
- [11] Wang G, Wen X, Wen J and Liu Y 2006 *J. Appl. Mech.* **73** 167
- [12] Smith D R, Pendry J B and Wiltshire M C K 2004 *Science* **305** 788
- [13] Djafari-Rouhani B, Dobrzynski L, Hardouin Duparc O, Camley R E and Maradudin A A 1983 *Phys. Rev. B* **28** 1711
- [14] Madelung O 1978 *Introduction to Solid-State Theory* (Berlin: Springer) chapter 2
- [15] Brillouin L 1953 *Wave Propagation in Periodic Structures* (New York: Dover) chapter 3
- [16] Ziolkowski R W 2004 *Phys. Rev. E* **70** 046608
- [17] Cummer S A and Schurig D 2006 *New J. Phys.* **9** 45
- [18] Cai L W and Sánchez-Dehesa S 2007 *New J. Phys.* **9** 450
- [19] Chen H Y and Chan C T 2007 *Appl. Phys. Lett.* **91** 183518
- [20] Cummer S A, Popa B, Schurig D, Smith D R, Pendry J, Rahm M and Starr A 2008 *Phys. Rev. Lett.* **100** 024301
- [21] Pendry J B, Schurig D and Smith D R 2006 *Science* **312** 1780
- [22] Milton G W, Briane M and Willis J R 2006 *New J. Phys.* **8** 248
- [23] Jensen J S 2003 *J. Sound Vib.* **266** 1053